Elemental imaging and petro-volcanological applications of an improved Laser Ablation Inductively Coupled Quadrupole Plasma Mass Spectrometry

Maurizio Petrelli [*], Daniele Morgavi, Francesco Vetere, Diego Perugini

Department of Physics and Geology, University of Perugia, Via A. Pascoli, 06123 Perugia, Italy

ARTICLE INFO

ABSTRACT

We report on the performance of the new Laser Ablation Inductively Coupled Plasma Mass Spectrometry instrumentation installed at the Department of Physics and Geology, University Perugia, empathizing its capabilities in elemental imaging, and the progresses in trace element and U/Pb geo-chronological determinations. The analytical device consists of a Thermo Fisher Scientific iCAP Q quadrupole mass spectrometer coupled with a Teledyne/ Photon Machine ArF Excimer G2 laser ablation system. Results on the reference material USGS BCR2G show that, in trace element configuration at 40 microns spot size, precision is better than 6.5% for all elements whereas accuracy is better than 10%. Results also show the improved precision with respect the X7+UP213 instrumentation in U/Pb geochronological studies. On this regard, concordia ages for the Plešovice and R33 zircons analyzed as unknowns are in close agreement with the accepted values. The potentials in 2D element imaging are also reported and successfully tested on a zoned plagioclase from the alkali basaltic Santa Venera lava Flow. Analytical data evidence that expanding the analysis to the second dimension will lead to more reliable and accurate results and it is going to open new prospective for the modeling of igneous systems.

Keywords: laser ablation; LA-ICP-MS; trace elements; U/Pb geochronology; elemental imaging; figures of merits.

INTRODUCTION

Laser Ablation Inductively Coupled Plasma Mass Spectrometry (LA-ICP-MS) is one of the most powerful micro-analytical technique for trace element and isotopic ratio determinations. Combining high spatial resolution with low limits of detection, it has been successfully applied in several fields like earth, natural and material sciences, biology, forensic, chemistry and industry (e.g. Norman et al., 1996; Jeffries et al., 1998; Norman et al., 1998; Becker and Dietze, 1999; Durrant, 1999; Günther et al., 1999; Horn et al., 2000; Sylvester, 2001; Kosler et al., 2002; Tiepolo, 2003; Tiepolo et al., 2003; Barca et al., 2007; Petrelli et al., 2007a; Petrelli et al., 2007b; Alagna et al., 2008; Barca et al., 2008; Petrelli et al., 2008; Sylvester, 2008; Barca et al., 2010; Barca et al., 2013; Pozebonet et al., 2014; Kimura et al., 2015). Elemental imaging by LA-ICP-MS is indeed a relative new application with, nowadays, a growing interest in the scientific community due to the great potentials in many fields (Rittner and Müller, 2011; Evans and Müller, 2013; Flórez et al., 2013; Paul et al., 2014). Examples of elemental imaging by LA-ICP-MS in Earth Sciences are reported by Evans and Müller (2013), Izmer et al. (2013) and Ubide et al. (2015) on carbonates (e.g., Foraminifera), impact spherule layers and mineral zoning respectively.

The operating principles of the LA-ICP-MS technique are basically unchanged since their introduction in 1985 (Gray, 1985) but, recently, significant improvements have been made in both laser ablation and ICP-MS instrumentations.

The commercial introduction of fast pulse (<4 ns) excimer lasers drastically increased the availability and diffusion of excimer laser ablation systems. As a consequence, excimer laser ablation systems are now a common tool in modern

PM

LA-ICP-MS laboratories. In addition, two-volume and fast response cells (e.g. ANU/Laurin Technic HelEx 2, New Wave Two volume 2 and the cell described by Fricker et al., 2011) greatly improved the efficiency of LA-ICP-MS systems combining the possibility of loading several samples with significant fast signal uptake and washout (Eggins et al., 1998; Müller et al., 2009; Fricker et al., 2011).

Modern ICP-MSs have been considerably improved in term of ion path geometry and plasma stability, resulting in a more efficient ion transmission through the instrument and a better neutrals removal. The result is an improved sensitivity and signal stability, leading to the acquisition of higher quality data.

The University of Perugia has hosted a LA-ICP-MS lab since 2004, here several analytical protocols for spatially resolved and bulk trace element determination of geological samples (Petrelli et al., 2007a; Petrelli et al., 2007b; Petrelli et al., 2008) and U/Pb geochronology on Zircons and Monazites (Alagna et al., 2008) have been created and developed. These protocols have been applied in order to resolve petrological to volcanological problems. Examples are the development of geochemical models (Perugini et al., 2006; Perugini et al., 2008; Piochi et al., 2009; Perugini et al., 2010), the analysis of melt and multiphase inclusions (Ferrando et al., 2009; Frezzotti et al., 2010) and the refining of geodynamic models (Gemelli et al., 2009).

In order to expand the capabilities of the present LA-ICP-MS laboratory and to develop new analytical protocols, the Department of Physics and Geology of the University of Perugia has recently acquired a new, high sensitivity quadrupole ICP-MS coupled with a fast pulse (<4 ns) excimer 193 nm Laser Ablation system.

In this work we report on the performance of the new LA-ICP-MS instrumentation empathizing its great versatility and the progresses over the previous LA-ICP-MS instrumentation in trace element and U/Pb geochronology. In particular, we present the capabilities of the new instrumentation in elemental imaging. This analytical protocol is not achievable in several LA-ICP-MS laboratories due to the long washout periods, characterizing common ablation cells, but can be readily applied using the new installed apparatus.

EXPERIMENTAL

The laser ablation device is a Teledyne/Photon Machine G2 equipped with a Two-Volume ANU (Australian National University) HelEx 2 cell. The laser source is an ATL-I-LS-R solid-state triggered excimer 193 nm laser. It is characterized by a maximum energy stabilized output of 12 mJ measured at the laser source. In the energy-stabilized configuration, it shows energy fluctuations of less than 2%, expressed as relative standard deviation (RSD). The

pulse duration is <4 ns resulting in more than 4 GW/cm^2 irradiance on the sample surface. The frequency can be varied from 1 to 300 Hz.

The beam delivery system is contained in a fully N$_2$-purged optical path to prevent ozone formation and concomitant energy loss on target. A rotating beam homogenizer, located before the beam shaper, guarantees the homogeneity of the laser beam along its surface.

The shape of the laser beam, on the sample surface, can be changed using two different devices. The first is the standard fast-change mask letting nominal circular spots of 1, 3, 4, 5, 8, 10, 12, 15, 20, 25, 30, 40, 50, 65, 85, 110, 130, 145, 155 microns in diameter and square spots with sizes of 5, 10, 20, 35, 80 and 150 microns. Cross shapes are also allowed, mainly for maintenance purposes. The second device that lets the shaping of the laser beam on the sample surface is a variable and rotating x-y-theta aperture. By using this device squared and rectangular spots of any size between 3 and 150 microns and any angular degree can be delivered to the sample surface. All spot sizes can be increased by a factor of 2 by using a beam-defocusing device.

The ablation cell design is based on the well know and extensively tested two volume HelEx cell developed at the Australian National University (ANU, Eggins et al., 1998; Woodhead et al., 2004) modified with an active flow in the funnel. The cell is provided with two different standard sample holders. The first hosts up to nine 1-inch and four ½-inch round samples (Figure 1a). The second hosts up to three 1-inch chips, four thin sections and two ½-inch round samples (Figure 1b). Different configurations for the sample holder can be designed and developed with little effort.

The coordinates of the spots to be analyzed can be manually arranged or automatically imported by using a text file containing the coordinates of all unknowns and two reference points.

The ablation is performed in Helium (He) atmosphere to enhance the ablation performance, to reduce particles deposition and inter-element fractionation (Eggins et al., 1998; Günther and Heinrich, 1999). Argon (Ar) and Nitrogen (N) are added after the ablation cell to reduce perturbations on the plasma torch and to enhance sensitivity (Hu et al., 2008). Tubing length from the ablation cell to the ICP-MS is reduced at its minimum (about 1 m) to reduce transport-related inter-element fractionation. A squid signal-smoothing device is located before the plasma torch to reduce signal spiking and to increase the stability of the signal (Müller et al., 2009).

The spectrometer is a quadrupole based Thermo Scientific iCAP Qc ICP-MS equipped with the high performance interface. It is capable of sensitivities above 10^6 cps/ppb for [110]In and [238]U, when operating in liquid solution mode with spray chamber nebulization, maintaining relative standard

deviations below 2% measured on 10 separate acquisitions of one minute each. In liquid solution mode, oxide formation measured as CeO^+/Ce^+ and double charged ions evaluated as Ba^{++}/Ba^+ are less than 2% and 3% respectively.

To evaluate figures of merits of the LA-ICP-MS (from now iCAP Q+G2), three different analytical setups are tested: 1) trace element analysis, 2) U/Pb geochronology on zircons and 3) trace element imaging. The operating condition of the ICP-MS and the specifications of each configuration are reported in Table 1.

LA-ICP-MS operating conditions are optimized before each analytical session and after any setup change by continuous ablation of NIST SRM 612 glass reference material (Pearce et al., 1997) in order to provide maximum
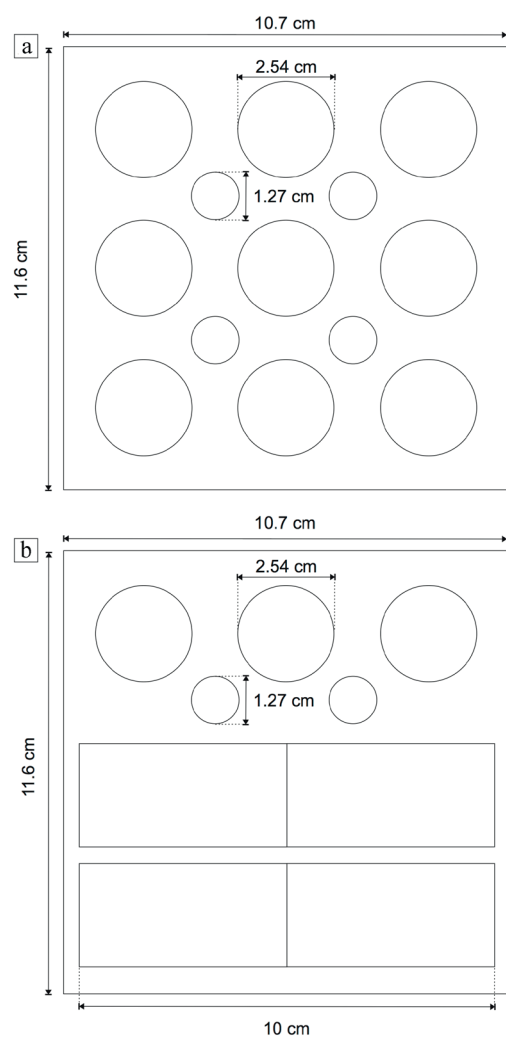

Figure 1. Schematic sketch of the two sample holders available for the iCAP Q+G2 instrumentation. The first (A) can load up to 9 and 4 round chips of 1 and ½ inches respectively. The second (B) can load thin sections, 3 round chips of 1 inches and 2 round chip of ½ inches.

Table 1. Laser Ablation and ICP-MS operating parameters.

ICP-MS	Thermo Fisher Scientific iCAP Q
RF power	1400-1550 W
Sampling depth	4.5-5.5 mm
Make Up gas flow (Ar)	0.55-0.75 l/min
Coolant gas flow (Ar)	14 l/min
Auxiliary gas flow (Ar)	0.8 l/min
Dwell time/mass	10-50 ms
Masses (m/z)	*Trace El., Imaging* ^{29}Si, ^{42}Ca, ^{45}Sc, ^{47}Ti, ^{51}V, ^{53}Cr, ^{59}Co, ^{85}Rb, ^{88}Sr, ^{89}Y, ^{90}Zr, ^{93}Nb, ^{133}Cs, ^{137}Ba, ^{139}La, ^{140}Ce, ^{141}Pr, ^{146}Nd, ^{147}Sm, ^{153}Eu, ^{157}Gd, ^{159}Tb, ^{163}Dy, ^{165}Ho, ^{166}Er, ^{169}Tm, ^{173}Yb, ^{175}Lu, ^{178}Hf, ^{181}Ta, ^{208}Pb, ^{232}Th, ^{238}U
	U/Pb ^{206}Pb, ^{207}Pb, ^{208}Pb, ^{232}Th, ^{238}U
Sampler, skimmer	Ni (with high sensitivity insert)
LA system:	Teledyne/Photon Machine G2
Fluence on target	0-12 J/cm^2
ThO$^+$/Th$^+$	<0.5 %
He gas flow - cell	0.4-0.8 l/min
He gas flow - funnel	0.2-0.4 l/min
N$_2$ gas flow	4-5 ml/min
Laser repetition rate	1-15 Hz
Transport tubing	<1.0 m

signal intensity and stability for the ions of interest, while suppressing oxides formation. The latter are monitored using ThO^+/Th^+ ratio. The U/Th ratio are also monitored and maintained close to 1. In detail, the trace element and imaging configurations are tuned by maximizing ^{42}Ca, ^{139}La and ^{232}Th, maintaining ThO^+/Th^+ below 0.5% and 0.9<U/Th<1.1. U/Pb mode is tuned by monitoring ^{208}Pb, ^{232}Th and ^{238}U, maintaining ThO^+/Th^+ below 0.5% and 0.9<U/Th<1.1.

The stability of the system is evaluated on ^{139}La, ^{208}Pb, ^{232}Th and ^{238}U by a short-term stability test. It consists of 5 acquisitions (one minute each) on a linear scan of NIST SRM 612 glass reference material.

RESULTS OF THE TUNING AND SENSITIVITIES OF THE ICAP Q+G2 LA-ICP-MS

Table 2 reports the typical ^{139}La, ^{208}Pb, ^{232}Th and ^{238}U values after the tuning of the iCAP Q+G2 instrumentation on a raster of 85 microns, 8 Hz, 3.5 J/cm^2 for trace element and imaging configuration. Under these operational conditions, representative values for the short-term stability, expressed as relative standard deviation, are below 2%.

Figure 2 reports the response curve obtained on a linear scan of NIST SRM 612 glass reference material with a velocity of 5 microns/seconds, a beam diameter of 40 microns, a frequency of 8 Hz and a fluence of 3.5 J/cm^2. Sensitivities for elements from Sc to Sr are between 5000 and 8000 cps/ppm. Mass above 88 Atomic Mass Unit (AMU) show higher sensitivities close to 10000 cps/ppm.

TIME RESOLVED SIGNALS

Figure 3a shows ^{139}La and ^{238}U signals acquired at 85 microns, 8 Hz and 3.5 J/cm^2. It is important to notice that the signal rises up in few milliseconds and it is constant and stable for the entire duration of the ablation. No significant inter element fractionation between ^{139}La and ^{238}U is observed. When the laser is switched off, a signal decay (washout) of more than 5 orders of magnitude occurs in less than 4 seconds. As a reference, time resolved signals for ^{139}La and

Table 2. Signal intensities for selected elements after the tuning at 85 microns, 8Hz and 3.5 J/cm^2.

Isotope	cps
^{139}La	1.11×10^6
^{208}Pb	0.60×10^6
^{232}Th	1.20×10^6
^{238}U	1.24×10^6

^{238}U obtained with a X7 ICP-MS coupled with a New Wave UP213 laser ablation system (from now X7+UP213, Petrelli et al., 2008) in close operating conditions is reported in Figure 3b. By comparing Figure 3a and 3b is clearly visible how the signal for the iCAP Q+G2 rises up faster, is higher and more stable than the one from the X7+UP213 instrumentation. Moreover, the complete washout of the signal occurs 5 times faster in the iCAP Q+G2 than in the X7+UP213. As we will show in the next paragraphs, all these features have a strong effect on the figure of merits of the applications reported in this manuscript (trace element determination, U/Pb geochronology and elemental imaging).

TRACE ELEMENTS ANALYSIS

Trace element determination by LA-ICP-MS is a widely used technique in petrology and volcanology. Some examples are the determination of partition coefficients in natural and experimental samples (Tiepolo et al., 2002), the study of mineral chemistry in plutonic and volcanic environment (Pearce et al., 1992; Davì et al., 2009), or the characterization of fluid, melt and multiphase inclusions (Frezzotti et al., 2010; Ferrando et al., 2009).

Analytical Protocol

The analytical protocol for trace element determination consists in the analysis of 10-15 samples, bracket by four determination of the NIST SRM612 reference material. The USGS BCR2G (Wilson, 1997) reference material is generally used as Quality Control. Data reduction is performed by using Iolite 3 (Paton et al., 2011) following identical protocol as in Longerich et al. (1996) and the analyzed isotopes are reported in Table 1. Each time resolved signal is carefully checked in order to exclude from trace element determinations portions that may be contaminated by inclusions and/or spurious peaks. ^{42}Ca is typically used as internal standard due to the reduced inter element fractionation if compared to ^{29}Si (Eggins et al., 1998). The latter is used as internal standard when ^{42}Ca is close or below its limit of detection.

Limits Of Detection (LODs)

In LA-ICP-MS LODs are function of the backgrounds and instrument's sensitivity. Specifically, they are function of the amount of material reaching the ICP-MS and, therefore, cubic function of the beam diameter.

Table 3 reports the LOD of the iCAP Q+G2 by using different spot sizes. LODs range between 0.002 (Th, U) and 1 (Cr) ppm, 0.001 (Th, U) and 0.5 (Cr) ppm, 0.0008 (Th) and 0.3 (Cr) ppm, 0.0002 (Th) and 0.3 (Cr) ppm and 0.00007 (Th) and 0.1 (Cr) ppm at 20, 30, 40, 65 and 85 microns for the laser beam diameter respectively on the BCR2G reference material at 8 Hz, 3.5 J/cm^2.

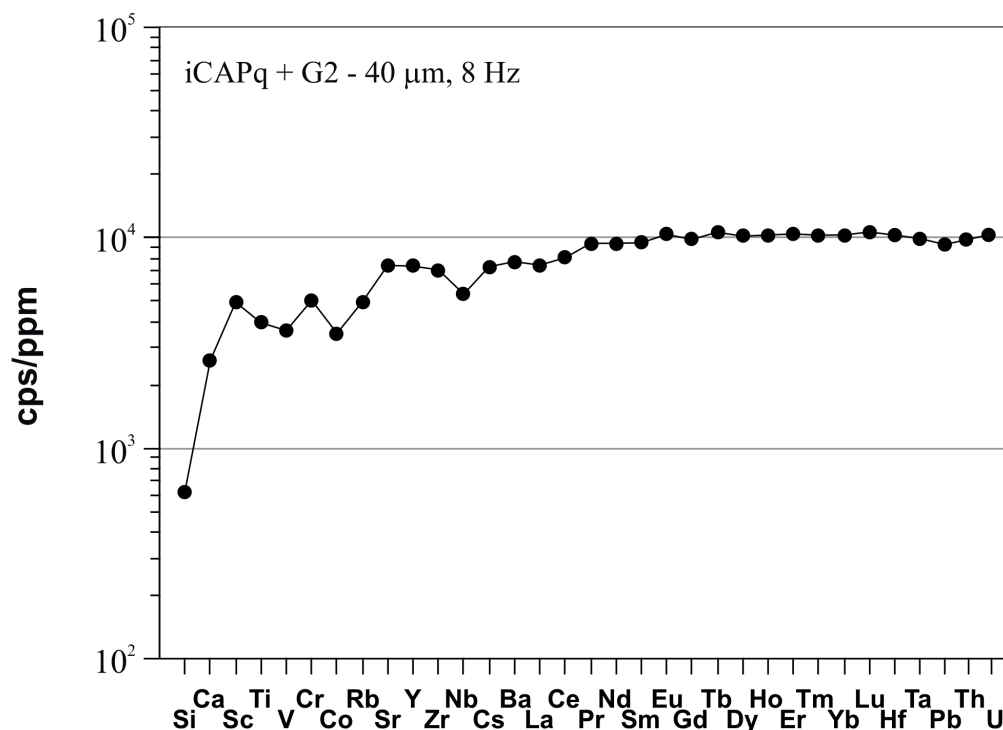In Figure 4 we illustrate the variations among LODs for a

Figure 2. Response curve at 40 microns, 8 Hz, 3.5 J/cm^2 for the iCAP Q+G2 instrumentation.

spot of 40 microns and 8 Hz obtained with the iCAP Q+G2 and X7+UP213 instrumentations. Figure 4 highlights the improvement in term of LODs for the iCAP Q+G2 compared with the X7+UP213. It is notable that detection limits at 40 microns are almost at the same order of magnitude of the ones reported by Tiepolo et al. (2003) obtained with a sector field ICP-MS.

Precisions and Accuracies in Trace Element Determinations

Precision and accuracies are evaluated on the USGS BCR2G reference material in two different analytical sessions consisting each of 6 determinations, using a spot size of 40 microns, a repetition rate of 8 Hz and a fluence of 3.5 J/cm^2 (Table 4, Figure 5). Figure 5 shows precisions, expressed as relative standard deviation, that are better than 6.5%, and accuracies, expressed as percent deviation from the recommended values, are better than 10% for all elements. Comparing the results reported in Petrelli et al. (2008) for the X7+UP213, we can assure that precision is greatly improved whereas accuracy is of the same order of magnitude. The improvement in precision is directly related with the increased sensitivity and signal stability of the iCAP Q+G2, as reported in Figure 3. Identical accuracy of the X7+UP213 is not surprising since it is directly related to the errors in the knowledge of the calibrator (NIST SRM612) and the reference material analyzed as unknown

(USGS BCR2G). In particular, the errors associated with the accepted values for the USGS BCR2G (Wilson, 1997) are of the same order of magnitude than those reported here.

U/PB GEOCHRONOLOGY ON ZIRCONS

U/Pb Geochronology on Zircons by LA-ICP-MS is continuously attracting the attention of researchers in Earth Science because it is cheaper and faster than other established micro-analytical techniques, such as Sensitive High Resolution Ion Microprobe (SHRIMP) and Secondary Ion Mass Spectrometry (SIMS). Providing a detailed list of the contributions reporting the successfully application of LA-ICP-MS U/Pb geochronology of zircons is outside the aim of this work and here we report on the capabilities of the iCAP Q+G2 in this field.

Analytical Protocol

The analytical protocol for U/Pb geo-chronology consists in the determinations of: (1) 6 calibration standards; (2) 10-15 unknown samples; (3) 6 calibration standards; (4) 2 quality control samples; (5) 10-15 unknown samples; (6) 6 calibration standards. Points (3), (4) and (5) can be replicated several times after the point (5) for the analysis of large zircon populations.

The 91500 zircon reference material is used as calibration standard (Wiedembeck et al., 1995) and the Plešovice
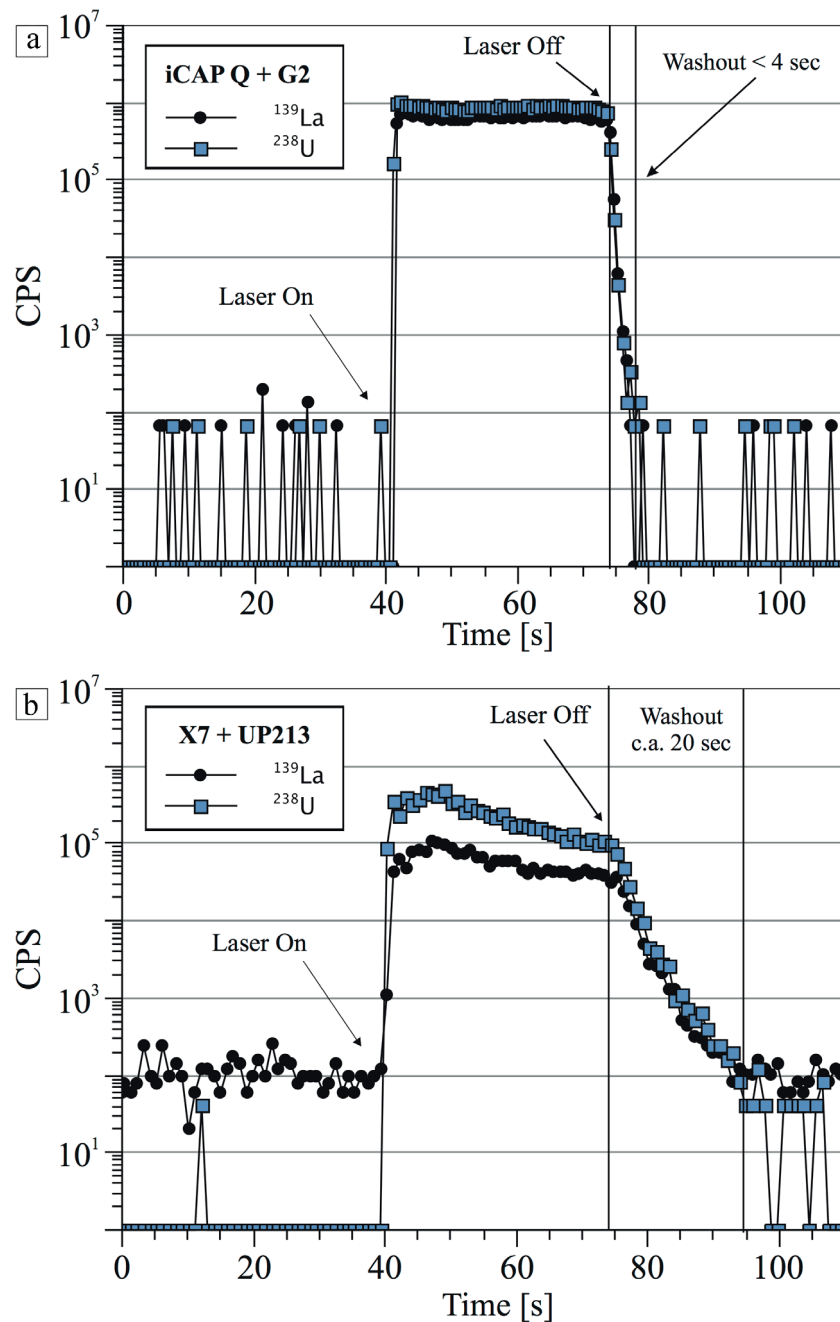
Figure 3. Time resolved signals for ^{139}La and ^{238}U for the two different configurations: a) iCAP Q+G2 ; b) X7+UP213.

(Slàma et al., 2008) and/or R33 (Black et al., 2004) zircons are utilized as quality control. The analyzed isostopes are reported in Table 1. Data reduction is performed by the Visual Age protocol reported by Petrus and Kamber (2012) in the Iolite 3 environment (Paton et al., 2011). In particular, raw signal counts and their ratios are carefully monitored in order to exclude from age calculations portions that may be contaminated by inclusions and/or spurious peaks. In additions, complex signals that may represent multiple ages have been carefully inspected in order to avoid misleading interpretations of the profiles. Net background-corrected count rates for each isotope are used for calculation. Data post-processing is performed using the Isoplot Excel macro (Ludwig K.R., 1980; 1998).

Table 3. Lower Limits of Detection at different spot dimensions. Laser operating conditions are fixed to 8 Hz, 3.5 J/cm^2.

	20 μm	30 μm	40 μm	65 μm	85 μm
Sc	0.2	0.1	0.06	0.04	0.02
Ti	0.5	0.3	0.2	0.1	0.05
V	0.08	0.04	0.03	0.02	0.01
Cr	1	0.5	0.3	0.3	0.1
Co	0.1	0.06	0.04	0.03	0.01
Rb	0.2	0.1	0.06	0.04	0.02
Sr	0.01	0.008	0.005	0.003	0.001
Y	0.05	0.02	0.02	0.01	0.00
Zr	0.03	0.01	0.009	0.006	0.003
Nb	0.05	0.03	0.01	0.01	0.01
Cs	0.02	0.01	0.007	0.005	0.002
Ba	0.09	0.07	0.03	0.02	0.01
La	0.008	0.005	0.003	0.002	0.001
Ce	0.003	0.002	0.001	0.001	0.0003
Pr	0.007	0.004	0.002	0.002	0.001
Nd	0.02	0.01	0.008	0.005	0.002
Sm	0.06	0.04	0.02	0.01	0.01
Eu	0.03	0.01	0.009	0.006	0.003
Gd	0.04	0.02	0.013	0.009	0.004
Tb	0.005	0.003	0.002	0.001	0.001
Dy	0.01	0.008	0.005	0.003	0.001
Ho	0.007	0.005	0.003	0.002	0.001
Er	0.01	0.008	0.005	0.003	0.002
Tm	0.006	0.003	0.002	0.001	0.001
Yb	0.02	0.01	0.007	0.004	0.002
Lu	0.003	0.002	0.001	0.001	0.000
Hf	0.02	0.01	0.008	0.005	0.002
Ta	0.003	0.002	0.001	0.001	0.0004
Pb	0.02	0.009	0.005	0.004	0.001
Th	0.002	0.001	0.001	0.0002	0.0007
U	0.002	0.001	0.001	0.0003	0.0001

PRECISIONS AND ACCURACIES IN U/PB GEOCHRONOLOGY

Results obtained using a spot of 20 microns, 8 Hz, 3.5 J/cm^2 are reported in Table 5 and Figure 6. In particular, Figure 6a shows the concordia diagram obtained for the 91500 reference material analyzed as unknown in two different analytical sessions and calibrated against different grains of the same 91500 reference material. These data represent an internal precision test for the instrumentation. As reference, Figure 6b shows the results obtained by

Alagna et al. (2008) on the 91550 zircon calibrated against itself using the X7+UP213 in the same operating conditions. Analyzing both Figure 6a and 6b clearly emerges that the internal precision is increased by a factor of 3 for ^{207}Pb/^{235}U and 1.5 for ^{206}Pb/^{238}U in the iCAP Q+G2 in respect to the X7+UP213. The accuracy of the U/Pb geochronology protocol is addressed analyzing the Plešovice and R33 zircons (Black et al., 2004; Slàma et al., 2008). The concordia diagrams for the R33 and Plešovice zircons are
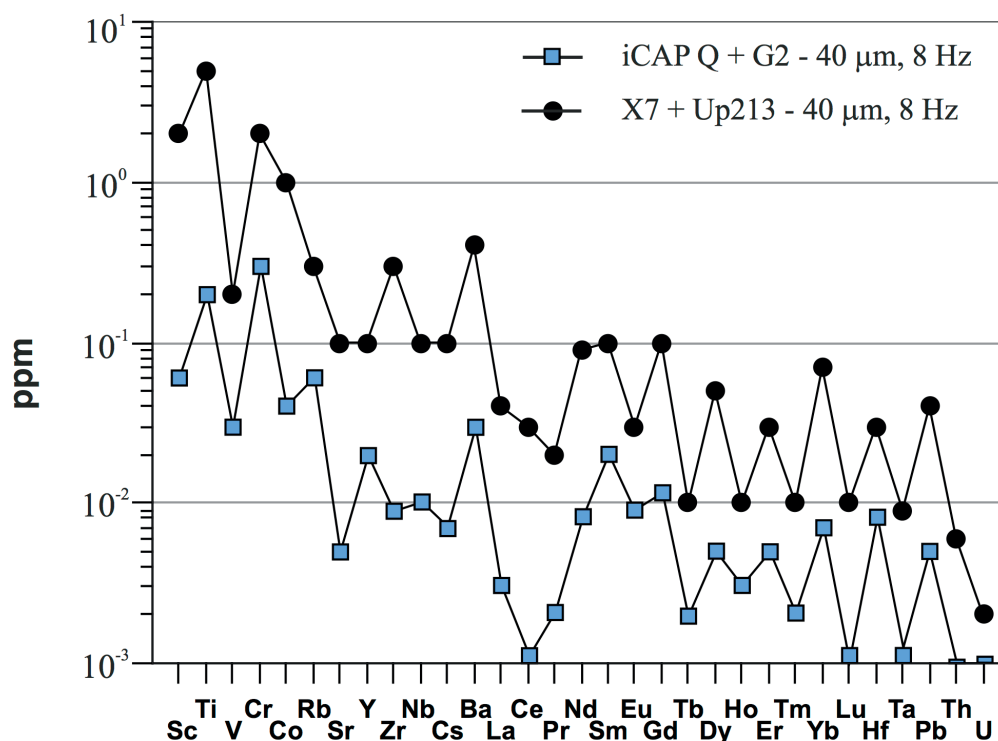
Figure 4. Limits of detection (LOD) in ppm for the iCAP Q + G2 and X7+UP213 instrumentations at 40 microns spot, 8 Hz.

reported in Figure 6c and 6d. Figure 6c and 6d show that the obtained concordia ages are in agreement with literature values of 419 Ma for the R33 and 337 Ma for the Plešovice (Slàma et al., 2008; Black et al., 2004). Figure 7 shows the esult of a 2-day stability test on the 91500 zircon reference material addressing the long-term reproducibility of the method.

TRACE ELEMENTS IMAGING BY LA-ICP-MS

In the last few years, trace elements imaging by LA-ICP-MS is becoming a major tool for analytical studies in Earth (Evans and Müller, 2013; Izmer et al., 2013) and Biologic (Becker et al., 2010) Sciences. In order to perform LA-ICP-MS imaging, a fast response cell is required (Evans and Müller, 2013). In particular, ablation cell design must be optimized to promote rapid uptake and washout times, avoiding cross-contamination of the laser-induced aerosol (Pisonero et al., 2013). The HelEx Cell installed in the iCAP Q+G2 instrumentation makes it an ideal tool for performing elemental imaging because of the quick uptake and washout times (Figure 3). Here we show the potentials of the iCAP Q+G2 in elemental imaging in geological samples performing a 2D map on a zoned plagioclase crystal occurring in the alkali basaltic Santa Venera lava flow (Mt. Etna; Perugini et al., 2003). It is notable that the same results could be obtained with a previous generation ICP-MS (e.g. Thermo X-series) if couple with a fast response ablation cell.

Analytical Protocol

Two main analytical approaches can be used for 2D imaging by LA-ICP-MS. The first consists in rastering the sample with a constant velocity along parallel lines (Becker et al., 2010). Images are the result of signal de-convolution against time. The second consists of square spots fired on a rectangular grid; each spot is then utilized as an image pixel. To evaluate the capabilities of the iCAP Q+G2 in elemental imaging, 1316 square spots of 16 microns were fired on a rectangular grid of 448 x 752 microns. Signals are then converted into images by an in-house developed python script (van Rossum and Drake, 2015). Regarding the integration settings, semi- and fully-quantitative data reductions can be performed. Semi-quantitative images only require the use of an external standard (e.g. NIST612) whereas fully-quantitative reductions needs the use of both an external standard coupled with an internal elemental standard. The concentration of the internal standard in the sample can be obtained using an alternative analytical method or from the known elemental stoichiometry when crystalline materials are analyzed (Longerich et al., 1996).

Table 4. LA-ICP-MS analyses for the USGS BCR2G glass performed at 40 microns, 8 Hz and 3.5 J/cm^2. For each laser beam diameter the average of 12 determinations ("This Study" column), the absolute standard deviation (1σ column) and the relative standard deviation (RSD column) are reported. The reference values from Wilson (1997) for the BCR2 are also reported.

	This Study (n =12)	1 σ	RSD	REF	Accuracy
Sc	33.6	0.8	2.4	33	1.8
Ti	13156	106	0.8	14100	-6.7
V	439	2	0.4	425	3.4
Cr	15.4	0.8	4.9	17	-9.4
Co	40.5	0.4	1.0	38	6.5
Rb	52	1	2.3	48	8.9
Sr	340	3	0.8	342	-0.7
Y	32.2	0.9	2.8	35	-7.9
Zr	173	4	2.2	184	-6.1
Nb	12.5	0.2	1.6	12.5	-0.3
Cs	1.26	0.04	3.1	1.16	8.9
Ba	693	5	0.7	683	1.4
La	24.7	0.3	1.1	24.7	0.2
Ce	53	1	1.8	53.3	0.3
Pr	6.5	0.1	2.2	6.7	-3.3
Nd	28.5	0.6	2.2	28.9	-1.4
Sm	6.7	0.3	4.0	6.59	0.9
Eu	1.9	0.1	5.7	1.97	-2.3
Gd	6.3	0.4	5.5	6.71	-5.7
Tb	0.96	0.03	3.4	1.02	-6.2
Dy	6.2	0.1	1.9	6.44	-4.5
Ho	1.24	0.03	2.6	1.27	-2.5
Er	3.4	0.1	3.7	3.7	-6.8
Tm	0.50	0.02	4.1	0.51	-2.2
Yb	3.3	0.2	6.3	3.39	-2.6
Lu	0.47	0.01	2.5	0.503	-7.2
Hf	4.6	0.1	2.6	4.84	-5.8
Ta	0.75	0.04	5.0	0.78	-3.8
Pb	11.4	0.4	3.8	11	3.3
Th	5.76	0.09	1.5	5.9	-2.3
U	1.73	0.05	3.1	1.69	2.6

Results and Discussion for Elemental Imaging

Figure 8 reports chemical maps for Ca, Ti, Nb, Ga, Rb, Y, Zr, Ba, Sm, Eu, Gd and Pb. Normalized concentrations clearly emphasize the zonation of the crystals and provide a quantitative estimation of the variation of each element within the crystal. The potential applications of 2D elemental maps by LA-ICP-MS are very large. They can be used, for example, to perform 2D models of diffusion to estimate the residence time of crystals in a magma chamber (e.g. Costa et al., 2003). On this regard, Costa et al. (2003), empathized that 1D diffusion study could lead to erroneous conclusions and wrong estimation of crystal residence times. In fact, the effects of two-dimensional diffusion become significant for relatively small and prismatic crystals; if this is ignored,
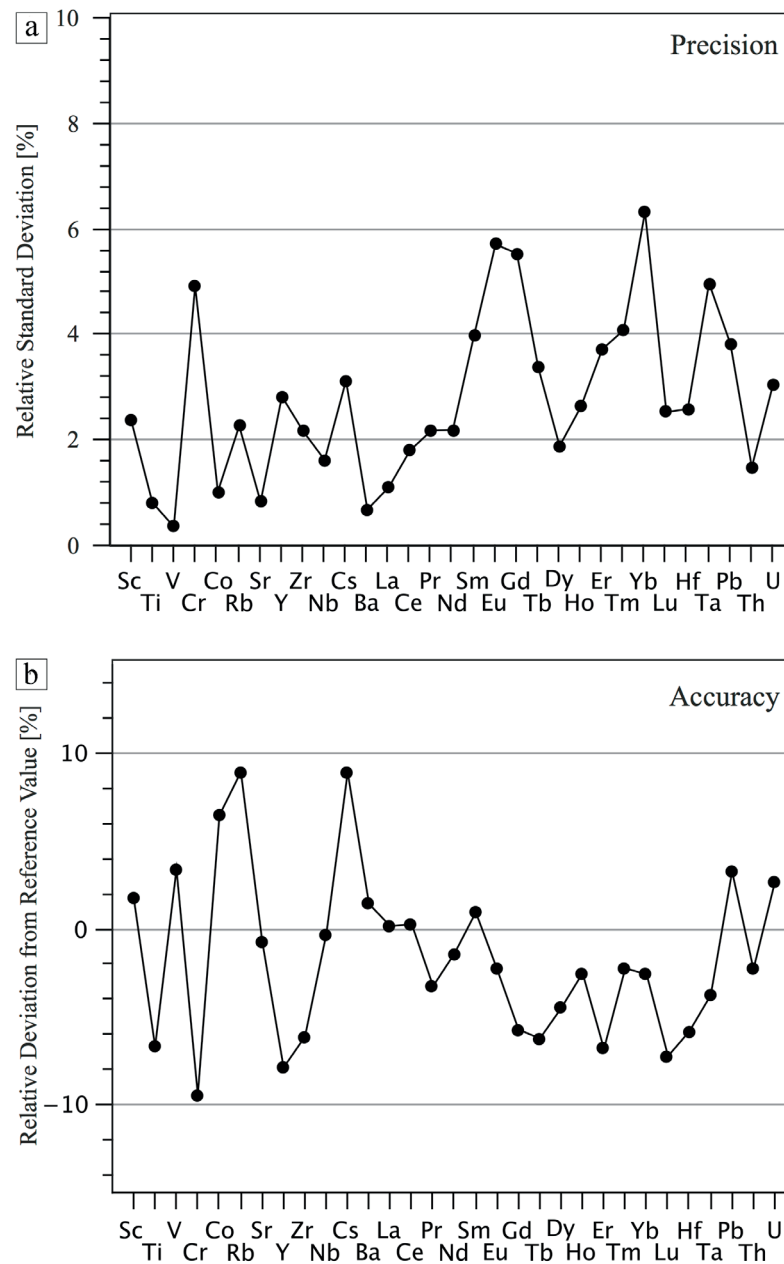
PM

Figure 5. Precision (a) and Accuracy (b) for the iCAP Q+G2 instrumentation at 40 microns spot, 8 Hz.

in spite of good fits to profile shapes, one would retrieve incorrect timescales (Costa et al., 2003). In addition, the knowledge of the spatial distribution of trace element within the crystals could help improving the accuracy of crystal/melt partition coefficients determination in natural and experimental studies. In detail, data plotted in Figure 8 can be used to give an estimation of the concentration of the melt in equilibrium with the grooving crystal and, therefore, of the evolution of the system. It is known that crystals can be used to estimate the chemical composition of the melt

during the crystallization process since they act as 'recorder' of chemical variations within the system (Triburzio et al., 2014). On this regard, it is important to note that the core and the rim areas of the crystal displayed in Figure 8 are not homogeneous and, therefore, data obtained from a single point or from a 1D transect can lead to erroneous result. Indeed, a systematic sampling of the system by using 2D chemical imaging will give a more precise and accurate estimation of the system.

Recently Ubide et al. (2015) showed how LA-ICP-MS

Table 5. LA-ICP-MS U/Pb data and calculated ages for zircon samples at 20 microns, 8 Hz and 3.5 J/cm^2.

|	Isotopic Ratios				Ages (Ma)			
Analyses	$^{207}Pb/^{235}U$	2σ	$^{206}Pb/^{238}U$	2σ	$^{207}Pb/^{235}U$	2σ	$^{206}Pb/^{238}U$	2σ
91500	1.843	0.035	0.180	0.002	1057	13	1065	13
91500	1.852	0.040	0.178	0.003	1062	14	1058	14
91500	1.846	0.054	0.181	0.003	1057	19	1071	16
91500	1.855	0.038	0.178	0.002	1063	14	1057	13
91500	1.852	0.035	0.180	0.002	1061	13	1066	13
91500	1.867	0.036	0.178	0.002	1064	13	1057	13
91500	1.842	0.034	0.180	0.003	1058	12	1067	14
91500	1.839	0.032	0.179	0.002	1057	12	1060	13
91500	1.843	0.035	0.180	0.002	1057	13	1065	13
91500	1.854	0.040	0.178	0.003	1063	14	1058	14
91500	1.847	0.055	0.181	0.003	1057	20	1070	16
91500	1.856	0.038	0.178	0.002	1063	14	1058	13
91500	1.853	0.035	0.180	0.002	1062	12	1067	13
91500	1.871	0.036	0.178	0.002	1066	13	1057	13
91500	1.842	0.034	0.180	0.003	1058	12	1067	14
91500	1.840	0.032	0.179	0.002	1057	12	1059	13
91500	1.858	0.042	0.178	0.003	1061	15	1054	15
91500	1.817	0.036	0.179	0.002	1048	13	1060	13
91500	1.858	0.035	0.180	0.002	1063	12	1064	13
91500	1.860	0.043	0.179	0.003	1063	15	1062	15
91500	1.856	0.039	0.180	0.003	1060	14	1066	15
91500	1.845	0.034	0.179	0.002	1057	12	1063	13
Plešovice	0.396	0.007	0.054	0.001	338	5	336	5
Plešovice	0.390	0.007	0.054	0.001	334	5	336	5
Plešovice	0.396	0.008	0.054	0.001	339	6	339	5
Plešovice	0.393	0.009	0.054	0.001	337	7	338	5
Plešovice	0.396	0.007	0.054	0.001	338	5	338	5
Plešovice	0.394	0.007	0.054	0.001	337	5	338	5
R33	0.527	0.027	0.068	0.001	428	18	423	8
R33	0.506	0.030	0.068	0.002	417	19	426	12
R33	0.519	0.018	0.068	0.001	423	12	424	7
R33	0.520	0.016	0.068	0.001	424	11	423	7
R33	0.528	0.019	0.067	0.001	427	13	421	7
R33	0.529	0.032	0.067	0.002	427	21	415	11

PM
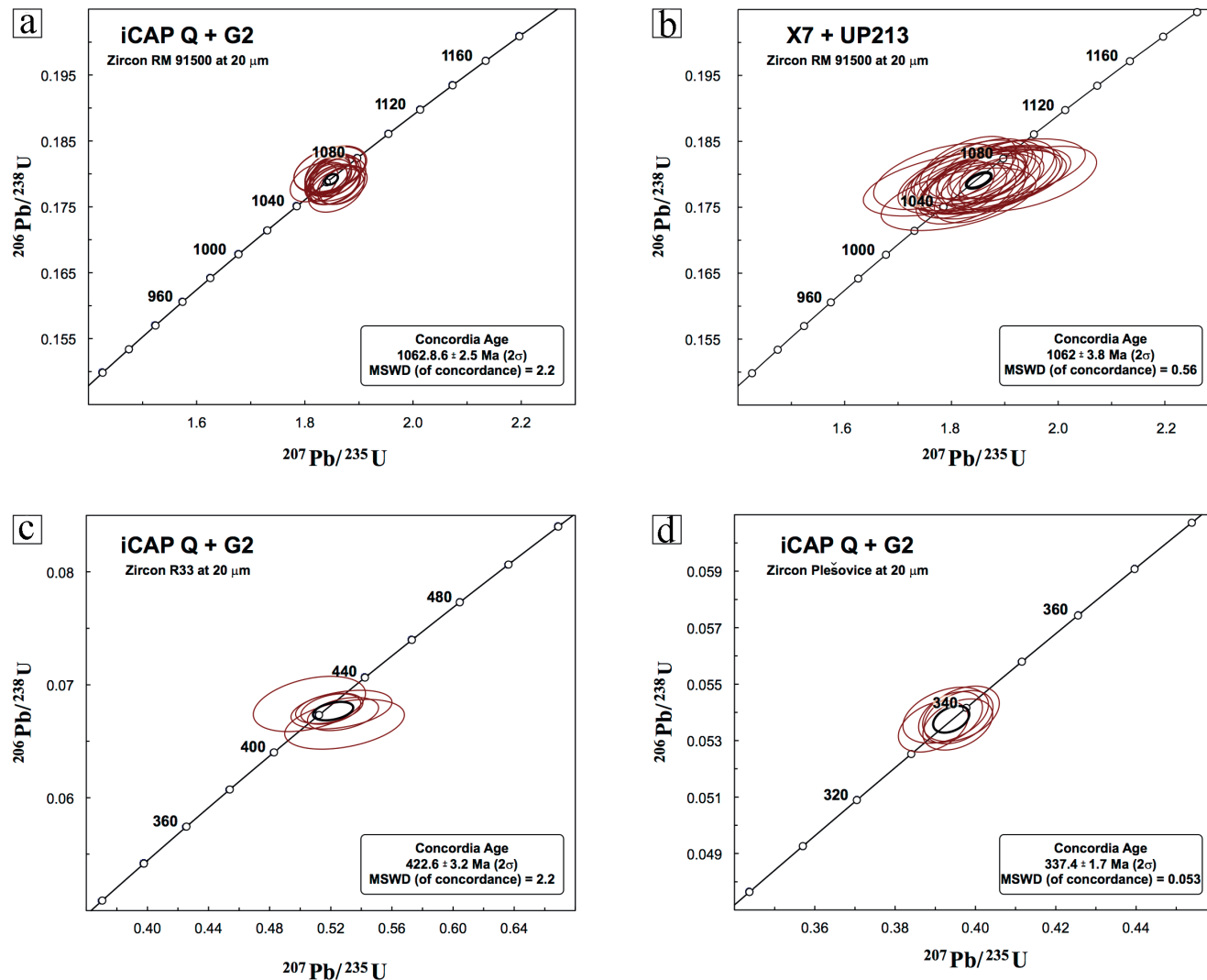
Figure 6. Concordia diagrams and Concordia ages: a) Zircon RM 91500 at 20 microns analyzed by the iCAP Q+G2; b) Zircon RM 91500 at 20 microns analyzed by the X7+UP213; c) Zircon R33 20 microns analyzed by the iCAP Q+G2; d) Zircon Plešovice at 20 microns analyzed by the iCAP Q+G2.

mapping has the potential to decipher magma history with unprecedented detail, by tracking compositional zoning at the trace element level. Ubide et al. (2015) analyzed several clinopyroxenes and amphiboles showing how they can be used to unravel spatio-temporal compositional variations of magmas in a porphyritic lamprophyre (Molí d'en Ponç, NE Spain) plumbing system, unraveling the history of magma pulses and magma evolution at depth.

CONCLUSIONS

The Thermo Fisher Scientific iCAP Q quadrupole mass spectrometer coupled with the Teledyne/Photon Machine ArF Excimer G2 laser ablation system allows high quality quantitative trace element analysis on geological samples and U/Pb age determinations on zircon coupling elevate

precision and accuracy. Results show that, in trace element configuration at 40 microns, precision is better than 6.5% whereas accuracy is better than 10%. Results also show improved precisions of the iCAP Q+G2 compared to the X7+UP213 in U/Pb geochronolgical studies. Therefore, concordia ages for the Plesovice and R33 Zircons analyzed as unknowns are in close agreement with the accepted values for these reference materials, highlighting the high accuracy of the method. The potentials in 2D element imaging are also reported and successfully tested on a zoned plagioclase from the alkali basaltic Santa Venera lava flow. Results evidence that expanding the analysis to the second dimension will lead to a more reliable and accurate results and it is going to open new prospective for the modeling of igneous systems.
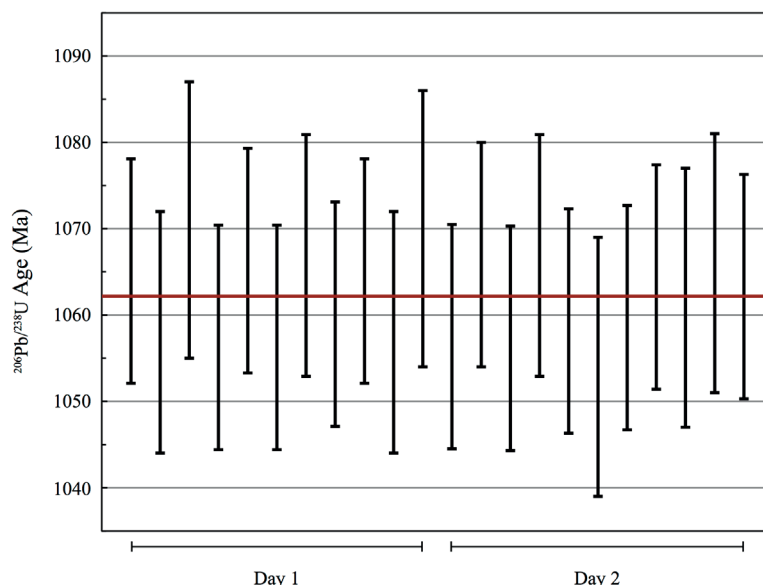
Figure 7. Long-term reproducibility test for U/Pb geo-chronology performed on the 91500 zircon reference material.
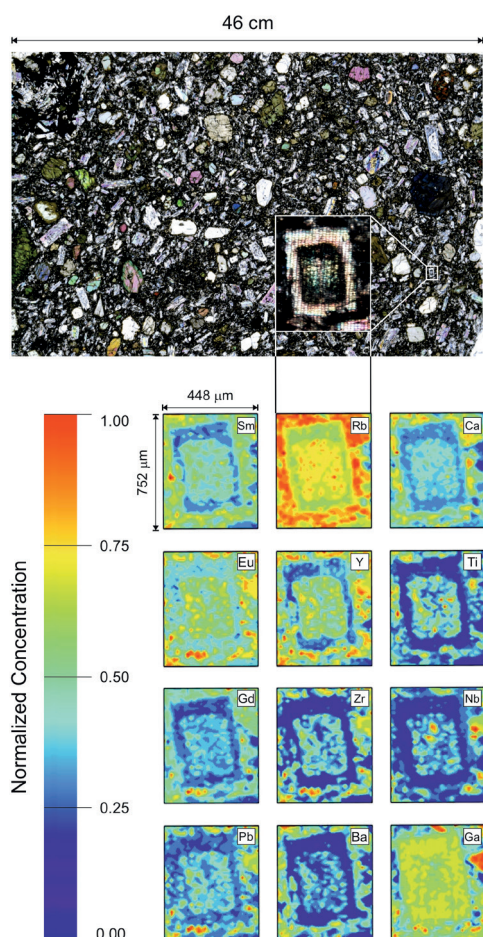

Figure 8. Chemical mapping of an area of 752 x 444 microns containing a zoned plagioclase from the alkali basaltic Santa Venera lava Flow (Mt. Etna).

REFERENCES

Alagna K.E., Petrelli M., Perugini D., Poli G. (2008) Micro-Analytical Zircon and Monazite U-Pb Isotope Dating by Laser Ablation-Inductively Coupled Plasma-Quadrupole Mass Spectrometry. Geostandards and Geoanalytical Research 32, 103-120.

Barca D., De Francesco A.M., Crisci G.M. (2007) Application of Laser Ablation ICP-MS for characterization of obsidian fragments from peri-Tyrrhenian area. Journal of Cultural Heritage 8, 141-150.

Barca D., De Francesco A.M., Crisci G.M., Tozzi C. (2008) Provenance of obsidian artifacts from site of Colle Cera, Italy, by LA-ICP-MS method. Periodico di Mineralogia 77, 41-42.

Barca D., Belfiore C.M., Crisci G.M., La Russa M.F., Pezzino A., Ruffolo S.A. (2010) Application of laser ablation ICP-MS and traditional techniques to the study of black crusts on building stones: A new methodological approach. Environmental Science and Pollution Research 17, 1433-1447.

Barca D., Miriello D., Pecci A., Barba L., Ortiz A., Manzanilla L.R., Blancas J., Crisci G.M. (2013) Provenance of glass shards in archaeological lime plasters by LA-ICP-MS: Implications for the ancient routes from the Gulf of Mexico to Teotihuacan in Central Mexico. Journal of Archaeological Science 40, 3999-4008.

Becker J.S. and Dietze H.J. (1999) Determination of trace elements in geological samples by laser ablation inductively coupled plasma mass spectrometry. Fresenius' Journal of Analytical

Chemistry 365, 429-434.

Becker J.S., Zoriy M., Matusch A., Wu B., Salber D., Palm C., Becker J. Susanne (2010) Bioimaging of metals by laser ablation inductively coupled plasma mass spectrometry (LA-ICP-MS). Mass Spectrometry Reviews 29, 156-175.

Black L.P., Kamo S.L., Allen C.M., Davis D.W., Aleinikoff J.N., Valley J.W., Mundil R., Campell I.H., Korsch R.J., Williams I.S., Foudoulis C. (2004) Improved 206Pb/238U microprobe geochronology by the monitoring of a trace-element-related matrix effect; SHRIMP, ID-TIMS, ELA-ICP-MS and oxygen isotope documentation for a series of zircon standards. Chemical Geology 205, 115-140.

Costa F., Chakraborty S., Dohmen R. (2003) Diffusion coupling between trace and major elements and a model for calculation of magma residence times using plagioclase. Geochimica et Cosmochimica Acta 67, 2189-2200.

Davì M., De Rosa R., Barca D. (2009) A LA-ICP-MS study of minerals in the Rocche Rosse magmatic enclaves: Evidence of a mafic input triggering the latest silicic eruption of Lipari Island (Aeolian Arc, Italy). Journal of Volcanology and Geothermal Research 182, 45-56.

Durrant S.F. (1999) Laser ablation inductively coupled plasma-mass spectrometry: Achievements, problems, prospects Journal of Analytical Atomic Spectrometry 14, 1385-1403.

Eggins S.M. (2005) In situ U-series dating by laser ablation multi-collector ICP-MS: New prospects for Quaternary geochronology. Quaternary Science Reviews 24, 2523-2538.

Eggins S.M., Kinsley L.P.J., Shelley J.M.G. (1998) Deposition and element fractionation processes during atmospheric pressure laser sampling for analysis by ICP-MS. Applied Surface Science 127-129, 278-286.

Evans D. and Müller W. (2013) LA-ICPMS elemental imaging of complex discontinuous carbonates: An example using large benthic foraminifera. Journal of Analytical Atomic Spectrometry 28, 1039-1044.

Ferrando S., Frezzotti M.L., Petrelli M., Compagnoni R. (2009) Metasomatism of continental crust during subduction: the UHP whiteschists from the Southern Dora-Maira Massif (Italian Western Alps). Journal of Metamorphic Geology 27, 739-756.

Flórez M.R., Aramendía M., Resano M., Lapeña A.C., Balcaen L., Vanhaecke F. (2013) Isotope ratio mapping by means of laser ablation-single collector-ICP-mass spectrometry: Zn tracer studies in thin sections of Daphnia magna. Journal of Analytical Atomic Spectrometry 28, 1005-1015.

Frezzotti M.L., Ferrando S., Peccerillo A., Petrelli M., Tecce F., Perucchi A. (2010) Chlorine- rich metasomatic H_2O-CO_2 fluids in amphibole-bearing peridotites from Injibara (Lake Tana region, Ethiopian plateau): Nature and evolution of volatiles in the mantle of a region of continental flood basalts. Geochimica et Cosmochimica Acta 74, 3023-3039.

Fricker M.B., Kutscher D., Aeschlimann B., Frommer J., Dietiker R., Bettmer J., Günther D. (2011) High spatial resolution trace element analysis by LA-ICP-MS using a novel ablation cell for multiple or large samples. International Journal of Mass Spectrometry 307, 39-45.

Gemelli M., Rocchi S., Di Vincenzo G., Petrelli M. (2009) Accretion of juvenile crust at the Early Palaeozoic Antarctic margin of Gondwana: geochemical and geochronological evidence from granulite xenoliths. Terra Nova 21, 151-161.

Gray A.L. (1985) Solid Sample introduction by laser ablation for

inductively coupled plasma source mass spectrometry. Analyst 110, 551-556.

Günther D. and Heinrich C.A. (1999) Enhanced sensitivity in laser ablation-ICP mass spectrometry using helium-argon mixtures as aerosol carrier. Journal of Analytical Atomic Spectrometry 14, 1363-1368.

Günther D., Jackson S.E., Longerich H.P. (1999) Laser ablation and ark/spark solid sample introduction into inductively coupled plasma mass spectrometers. Spectrochimica Acta 54B, 381-409.

Horn I., Rudnick R.L., Mcdonough W.F. (2000) Precise elemental and isotope ratio determination by simultaneous solution nebulization and laser ablation ICP-MS: Application to U-Pb geochronology. Chemical Geology 167, 405-425.

Hu Z., Gao S., Liu Y., Hu S., Chen H., Yuan H. (2008) Signal enhancement in laser ablation ICP-MS by addition of nitrogen in the central channel gas. Journal of Analytical Atomic Spectrometry 23, 1093-1101.

Izmer A., Goderis S., Simonson B.M., Mcdonald I., Hassler S.W., Claeysb P., Vanhaecke F. (2013) Application of laser ablation-ICP-mass spectrometry for 2-dimensional mapping of element distributions in a Late Archean impact spherule layer. Journal of Analytical Atomic Spectrometry 2013, 28, 1031.

Jeffries T.E., Jackson S.E., Longerich H.P. (1998) Application of a frequency quintupled Nd:YAG (λ=213 nm) for laser ablation inductively coupled plasma mass spectrometric analysis of minerals. Journal of Analytical Atomic Spectrometry 13, 935-940.

Kimura J.I., Chang Q., Itano K., Iizuka T., Vaglarova S., Tanic K. (2015) An improved U-Pb age dating method for zircon and monazite using 200/266 nm femtosecond laser ablation and enhanced sensitivity multiple-Faraday collector inductively coupled plasma mass spectrometry. Journal of Analytical Atomic Spectrometry 30, 494-505.

Kosler J., Fonneland H., Sylvester P.J., Tubrett M.N., Pedersen R.B. (2002) U-Pb dating of detrital zircons for sediment provenance studies-a comparison of laser ablation ICPMS and SIMS technique. Chemical Geology 182, 605-618.

Longerich H.P., Jackson S.E., Günther D. (1996) Laser ablation inductively coupled plasma mass spectrometric transient signal data acquisition and analyte concentration calculation. Journal of Analytical Atomic Spectrometry 11, 899-904.

Ludwig K.R. (1980) Calculation of uncertainties of U-Pb isotope data. Earth and Planetary Science Letters 46, 212-220.

Ludwig K.R. (1998) On the treatment of concordant uranium-lead ages. Geochimica et Cosmochimica Acta 62, 665-676.

Müller W., Shelley M., Miller P., Broude S. (2009) Initial performance metrics of a new custom-designed ArF excimer LA-ICPMS system coupled to a two-volume laser-ablation cell. Journal of Analytical Atomic Spectrometry 24, 209-214.

Norman M.D., Pearson N.J., Sharma A., Griffin W.L. (1996) Quantitative analysis of trace elements in geological materials by laser ablation icp-ms: instrumental operating conditions and calibration values of nist glasses. Geostandards Newsletter 20, 247-261.

Norman M.D., Griffin W.L., Pearson N.J., Garcia M.O., O'reilly S.Y. (1998) Quantitative analysis of trace elements abundances in glasses and minerals: a comparison of laser ablation inductively coupled plasma mass spectrometry, solution inductively coupled plasma mass spectrometry, proton

microprobe and electron microprobe data. Journal of Analytical Atomic Spectrometry 13, 477-482.

Paton C., Hellstrom J., Paul B.,Woodhead J., Hergt J. (2011) Iolite: Freeware for the visualisation and processing of mass spectrometric data. Journal of Analytical Atomic Spectrometry 26, 2508-2518.

Paul B., Woodhead J.D., Paton C., Hergt J.M., Hellstrom J., Norris C.A. (2014) Towards a Method for Quantitative LA-ICP-MS Imaging of Multi-Phase Assemblages: Mineral Identification and Analysis Correction Procedures. Geostandards and Geoanalytical Research 14, 253-263.

Pearce N.J.G., Perkins W.T., Abell I., Duller G.A.T., Fuge R. (1992) Mineral microanalysis by laser ablation inductively coupled plasma mass spectrometry. Journal of Analytical Atomic Spectrometry 19927, 53-57.

Pearce J.G.N., Perkins W.T., Westgate J.A., Gorton M.P., Jackson S.E., Neal C.R., Chenery S.P. (1997) A compilation of new and published major and trace element data for NIST SRM 610 and NIST SRM 612 glass reference materials. Geostandards Newsletter 21, 115-144.

Perugini D., Busà T., Poli G., Nazzareni S. (2003) The Role of Chaotic Dynamics and Flow Fields in the Development of Disequilibrium Textures in Volcanic Rocks. Journal of Petrology 44, 733-756.

Perugini D., Petrelli M., Poli G. (2006) Diffusive fractionation of trace elements by chaotic mixing of magmas. Earth and Planetary Science Letters 243, 669-680.

Perugini D., De Campos C.P., Dingwell D.B., Petrelli M., Poli G. (2008) Trace element mobility during magma mixing: preliminary experimental results. Chemical Geology 256, 146-157.

Perugini D., Poli G., Petrelli M., De Campos C.P., Dingwell D.B. (2010) Time-scales of recent Phlegrean Fields eruptions inferred from the application of a 'diffusive fractionation' model of trace elements. Bulletin of Volcanology 72, 431-447.

Petrelli M., Perugini D., Poli G., Peccerillo A. (2007a) Graphite electrode lithium tetraborate fusion for trace element determination in bulk geological samples by laser ablation ICP-MS. Microchimica Acta 158, 275-282.

Petrelli M., Caricchi L., Ulmer P. (2007b) Application of High Spatial Resolution Laser Ablation ICP-MS to Crystal-Melt Trace Element Partition Coefficient Determination. Geostandards and Geoanalytical Research 31, 13-25.

Petrelli M., Perugini D., Alagna K.E., Poli G., Peccerillo A. (2008) Spatially resolved and bulk trace element analysis by laser ablation-inductively coupled plasma-mass spectrometry (LA-ICP-MS). Periodico di Mineralogia 77, 3-21.

Petrus J.A. and Kamber B.S. (2012) VizualAge: a novel approach to LA-ICP-MS U-Pb geochronology. Geostandards and Geoanalytical Research 36, 247-270.

Piochi M., De Astis G., Petrelli M., Ventura G., Sulpizio R., Zanetti A. (2009) Constraining the recent plumbing system of Vulcano (Aeolian Arc, Italy) by textural, petrological, and fractal analysis: The 1739 AD Pietre Cotte lava flow. Geochemistry, Geophysics, Geosystems 10, doi: 10.1029/2008GC002176.

Pisonero J., Bordela N., Smentkowskib V.S. (2013) Elemental imaging. Journal of Analytical Atomic Spectrometry 2013, 970-972.

Pozebon D., Scheffler G.L., Dressler V.L., Nunes M.A.G. (2014) Review of the applications of laser ablation inductively coupled plasma mass spectrometry (LA-ICP-MS) to the analysis of biological samples. Journal of Analytical Atomic Spectrometry 29, 2204-2228.

Rittner M. and Muller W. (2011) 2D mapping of LAICPMS trace element distributions using R. Computers & Geosciences 42, 152-161.

SláMa J., KošLer J., Condon D.J., Crowley J.L., Gerdes A., Hancharg J.M., Horstwoodd M.S.A., Morrish G.A., Nasdalai L., Norberg N., Schaltegger U., Schoene B., Tubrett M.N., Whitehouse M.J. (2008) Plešovice zircon - A new natural reference material for U-Pb and Hf isotopic microanalysis. Chemical Geology 249, 1-35.

Sylvester P. (2001) Laser Ablation ICP-MS in the Earth Sciences: Principles and applications. Mineralogical Association Canada Short Course Series 29, 243 pp.

Sylvester P. (2008) Laser Ablation ICP-MS in the Earth Sciences: Current Practices and Outstanding Issues. Mineralogical Association Canada Short Course Series 40, 356 pp.

Tiepolo M., Oberti R., Vannucci R. (2002) Trace-element incorporation in titanite: constraints from experimentally determined solid/liquid partition coefficients. Chemical Geology 191, 105-119.

Tiepolo M. (2003) In situ Pb geochronology of zircon with laser ablation- inductively coupled plasma-sector field mass spectrometry. Chemical Geology 199, 159-177.

Tiepolo M., Bottazzi P., Palenzona M., Vannucci R. (2003) A laser probe couplet with ICP-double focusing sector-field mass spectrometer for in situ analysis of geological samples and U-Pb dating of zircon. Canadian Mineralogist 41, 259-272.

Tribuzio R., Renna M.R., Dallai L., Zanetti A. (2014) The magmatic-hydrothermal transition in the lower oceanic crust: Clues from the Ligurian ophiolites, Italy. Geochimica et Cosmochimica Acta 130, 188-211.

Ubide T., McKenna C.A., Chew D.M., Kamber B.S. (2015) High-resolution LA-ICP-MS trace element mapping of igneous minerals: In search of magma histories. Chemical Geology 409, 157-168.

Van Rossum G. and Drake F.L.Jr. (2015) The python library reference - release 2.7.10. python software foundation, https:// docs.python.org/2.7/download.html

Wiedenbeck M., Allé P., Corfu F., Griffin W.L., Meier M., Oberli F., Von Quadt A., Roddick J.C., Spiegel W. (1995) Three natural zircon standards for U-Th-Pb, Lu-Hf, trace element and REE analyses. Geostandards Newsletter 19, 1-23.

Wilson S.A. (1997) The collection, preparation, and testing of USGS reference material BCR-2, Columbia River, Basalt. U.S. Geological Survey Open-File Report 98.

Woodhead J., Hergt J., Shelley M., Eggins S., Kemp R. (2004) Zircon Hf-isotope analysis with an excimer laser, depth profiling, ablation of complex geometries, and concomitant age estimation. Chemical Geology 1, 121-135.